Supporting Information

2D Layered Semiconducting $(LCu_3I_3)_n$ Coordination Polymer for Energy Storage through Dual Ion Intercalation

Dilip Pandey[a†], Mayank K. Singh[b†], Shivendu Mishra[a], Dhirendra K. Rai*[b], Abhinav Raghuvanshi*[a]

[a]*Department of Chemistry, Indian Institute of Technology Indore, Simrol, Indore, Madhya Pradesh, 453552, India.*

[b]*Sustainable Energy and Environmental Materials (SEEM) Lab, Department of Metallurgical Engineering and Material Science, Indian Institute of Technology Indore, Simrol, Indore, Madhya Pradesh, 453552, India.*

Email- r.abhinav@iiti.ac.in (AR) ; dkrai@iiti.ac.in (DKR)

Table of contents

General Information

Materials

Materials required for the synthesis of ligands such as 1,3,5-trithiane (>99%) bought from TCI (India) and used without further purification. We purchased CuI (>99%) from Loba Chemie Pvt. Ltd. and acetonitrile HPLC grade from Finar Chemicals Pvt. Ltd.

Characterization:

Single crystal measurements of **CuI-CP** were conducted using a suitable crystal on a SuperNova diffractometer. The diffraction data were collected at ambient temperature at 298 K utilizing Mo Kα radiation that was monochromatized with graphite (λ = 0.7107 Å) at 50 kV and 30 mA. Using Olex2[1], the structure was solved with the SHELXT structure solution program using Intrinsic Phasing and refined with the SHELXL refinement package using Least Squares minimization.[1,2]

Experimental Section

Electrode Fabrication for Electrochemical Analysis

Initially, slurries were prepared using ultrasonication to disperse 10 mg of electrode materials in 1 mL of ethanol for 2 hours. At the same time, sections of carbon paper (CP) measuring 2x1 cm^2 were cut and thoroughly cleaned for subsequent use. Subsequently, the as-prepared slurry was evenly dropcasted on 1x1 cm of carbon paper and dried in a vacuum for 4 hours. For all electrochemical tests, a 1 M potassium hydroxide (KOH) electrolyte solution was used.

Electrochemical studies

Charge storage study: Electrochemical studies were performed using a NOVA software-controlled Autolab PGSTAT 204N. The reference electrode employed was Ag/AgCl, the counter electrode was made of platinum, and the working electrode consisted of carbon paper

coated with the electrode material. The experiments included cyclic voltammetry (CV) at various scan rates and galvanostatic charge/discharge (GCD) at different current densities using an electrochemical workstation. Electrochemical impedance spectroscopy (EIS) was also carried out with a 10 mV AC amplitude over a frequency range spanning from 10 mHz to 100 kHz. The following equation was used to determine the specific capacity using the GCD discharge curve.

$$C = \frac{I\,\Delta t}{m} \tag{1}$$

where I is the current, Δt is the discharge time, and m is the mass of the coated active material.

Fabricating symmetrical solid-state device:

A Swagelok cell having a 16 mm diameter was utilized for fabricating a solid-state symmetrical charge storage device. An electrode slurry was synthesized by subjecting 10 mg of electrode materials to sonication in a 1 mL ethanol solution for a period of 2 h. This resulting slurry was then dropcasted to a circular Ni-foam substrate and subsequently placed in an oven at 60 °C for 8 h to ensure proper drying. The electrolyte solution was prepared in 1g of PVA in 10 mL water. This mixture was then heated at 90 °C with continuous stirring for 3 h, to which 10 mL of a 1M KOH solution was added. Following this step, cellulose paper as a separator was soaked into the resulting PVA-KOH gel electrolyte. Subsequently, the separator was sandwiched by two electrode material-coated Ni-foam and assembled in a Swagelok cell to fabricate a symmetrical supercapacitor device.

From the GCD curves, the following equations were used to derive the fabricated device's specific capacity, energy density (E), and power density (P).

$$C = \frac{2I\,\Delta t}{m} \tag{2}$$

$$E\left(\frac{Wh}{kg}\right) = \frac{0.5 \times C\Delta V}{3.6} \quad (3)$$

$$P\left(\frac{W}{kg}\right) = \frac{3600 \times E}{\Delta t} \quad (4)$$

active material mass (g), discharge time (s), current (A), potential window (ΔV), and specific capacity (C g^{-1}).

Theoretical Capacity:- We have calculated the theoretical specific capacity using:-

Capacity, C = nF/M

Where n is the number of electron transfers,

F is Faraday Constant,

M is Molar mass,

For one formula unit of CH_2CuIS, the formula weight is 236.53 g/mol. Considering CuI-CP undergoes a two-electron transfer, the calculated specific capacity is 815 C g^{-1}.

Table S1. Crystallographic parameters of **CuI-CP**

Compound	**CuI-CP**
CCDC No.	2289195
Formula	CH2CuIS
Formula Weight	236.53
Wavelength	0.71073 Å
Crystal System	trigonal
Space group	R3
a/Å	7.2224(3)
b/ Å	7.2224(3)
c/ Å	20.6643(11)
α /°	90
β/°	90
γ/°	120
V/ $Å^3$	933.50(9)
Z	9
$ρ_{calcd}$ (g/cm^3)	3.787
Temperature/K	298
GOF	1.101

2θ range for data collection	6.806 to 54.946
Reflections collected	2329
Independent reflections	926 [R_{int} = 0.062]
Completeness to θ=25.242	99.6
Final R indices [I>2σ(I)]	R_1 = 0.0413 , wR_2 = 0.1091
Final R indices [all data]	R_1 = 0.0417 , wR_2 = 0.1095
Largest diff. peak/hole/ e Å^{-3}	1.17/-1.21

Table S2. Important bond lengths (Å).

I1-Cu1[1]	2.655(2)
I1-Cu1	2.655(2)
I1-Cu1[2]	2.655(2)
I2-Cu1[3]	2.601(2)
I2-Cu1[4]	2.601(2)
I2-Cu1	2.601(2)
I3-Cu1[5]	2.719(2)
I3-Cu1	2.719(2)
I3-Cu1[6]	2.719(2)
Cu1-S1	2.306(4)
S1-C1[3]	1.816(16)
S1-C1	1.819(16)
C1-S1[4]	1.816(16)

Symmetry operation code- [1]2-y,1+x-y,+y; [2]1+y-x,2-x,+z; [3]1-y,1+x-y,+z; [4]+y-x,1-x,+z; [5]1+y-x,1-x,+z; [6]1-y,+x-y,+z

Table S3. Selected bond angles (˚).

Cu1[1]-I1-Cu1	110.34(6)

Cu1[1]-I1-Cu1[2]	110.35(6)
Cu1-I1-Cu1[2]	110.34(6)
Cu1[3]-I2-Cu1[4]	85.35(7)
Cu1[4]-I2-Cu1	85.35(7)
Cu1[3]-I2-Cu1	85.35(7)
Cu1[5]-I3-Cu1[6]	119.84(8)
Cu1[6]-I3-Cu1	119.84(8)
Cu1[5]-I3-Cu1	119.84(8)
I1-Cu1-I3	103.98(7)
I2-Cu1-I1	107.58(8)
S1-Cu1-I1	112.93(8)
S1-Cu1-I2	110.91(13)
S1-Cu1-I3	122.18(13)
C1[3]-S1-Cu1	97.97(12)
C1-S1-Cu1	116.70(5)
C1[3]-S1-C1	112.10(6)
S1[4]-C1-S1	98.60(4)

Symmetry operation code- [1] - *x*, 1 - *y*, - *z*; [2] + *x*, 1 + *y*, - 1 + *z*; [3] + *x*, 1 + *y*, + *z*; [4] + *x*, - 1 + *y*, 1 + *z*; [5] + *x*, - 1 + *y*, + *z*

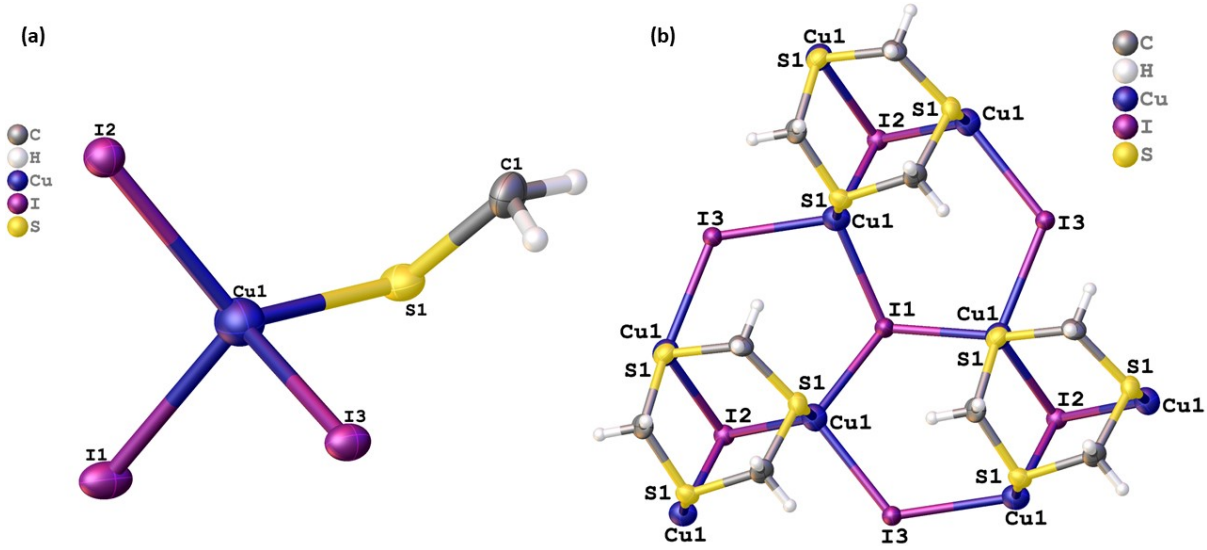

Figure. S1 (a) Asymmetric unit of the 2D **CuI -CP**, (b) different coordination mode of Cu and I ions in chain propagation.

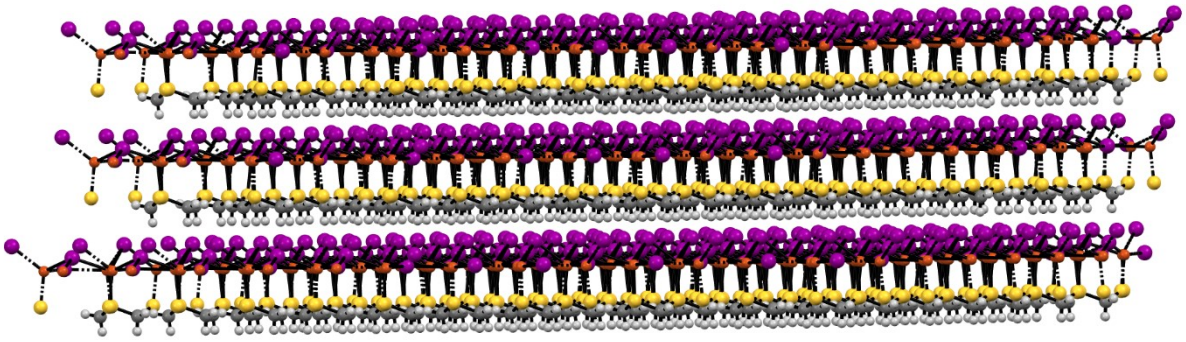

Figure S2. Crystal structure arrangement of **CuI-CP** with different layers.

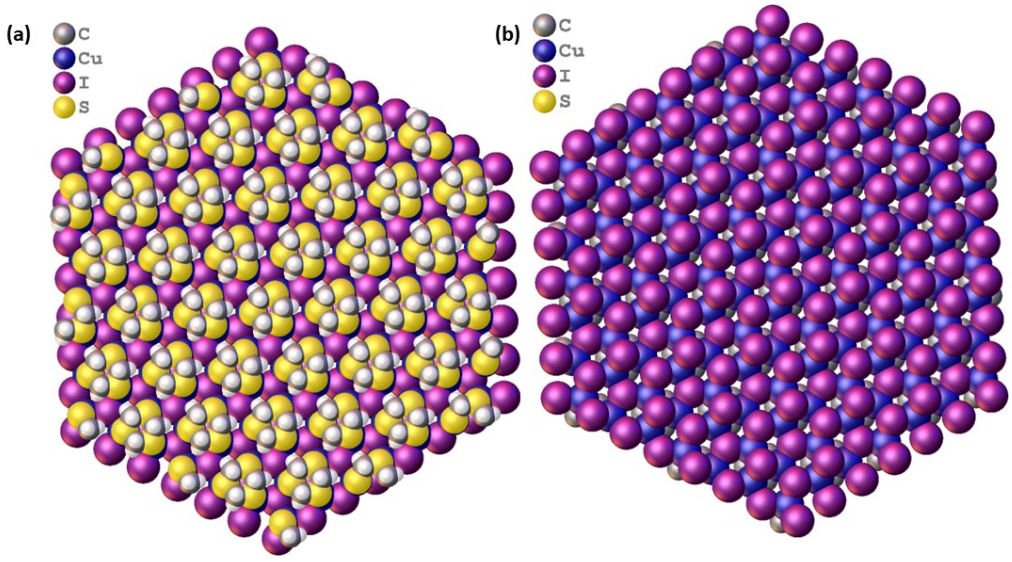

Figure S3. (a) The space fill model of **CuI-CP** along the a-axis, (b) space fill model along the b-axis.

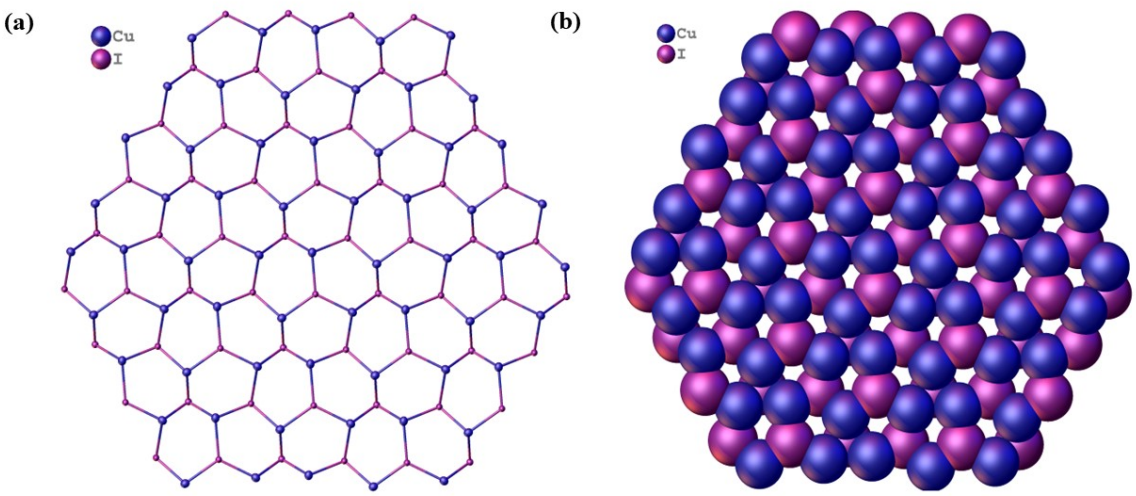

Figure S4. Continuous Cu-I 2D sheet framework in (a) ellipsoid and (b) space-filled model.

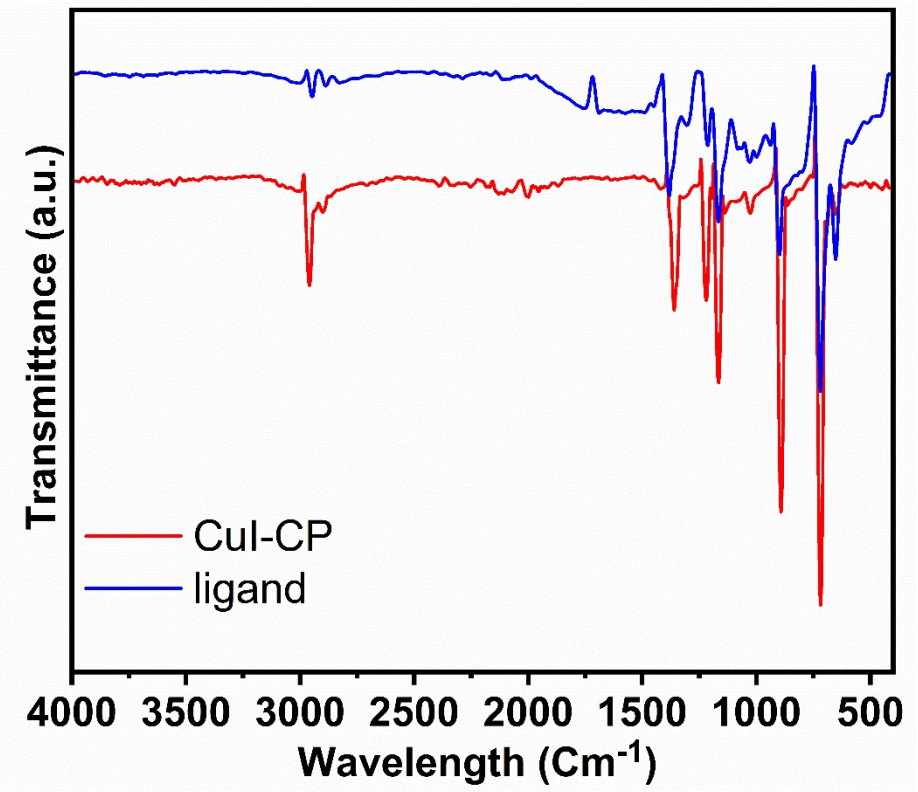

Figure S5. IR spectra of ligand and **CuI-CP**.

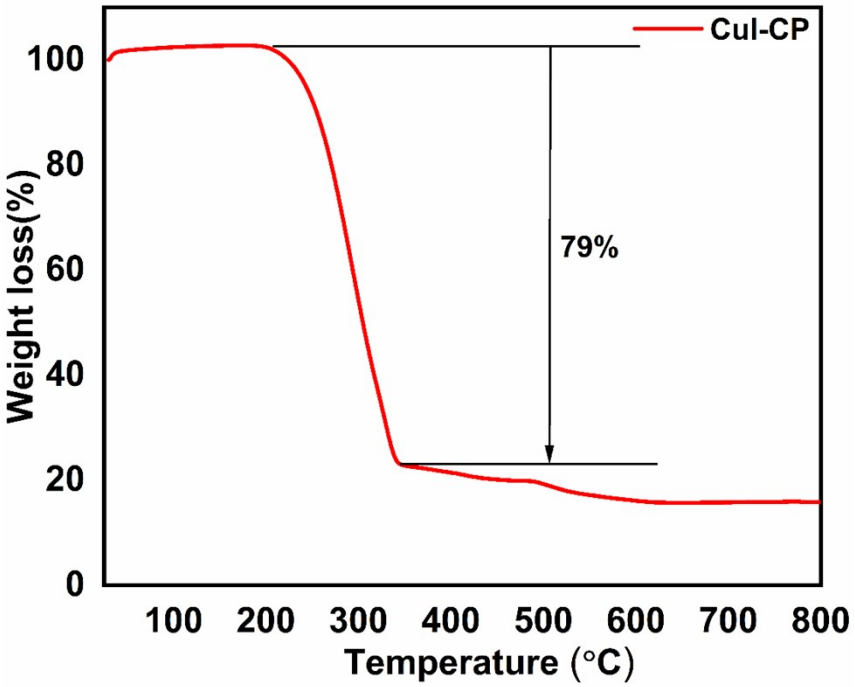

Figure S6. TGA curve of **CuI-CP**.

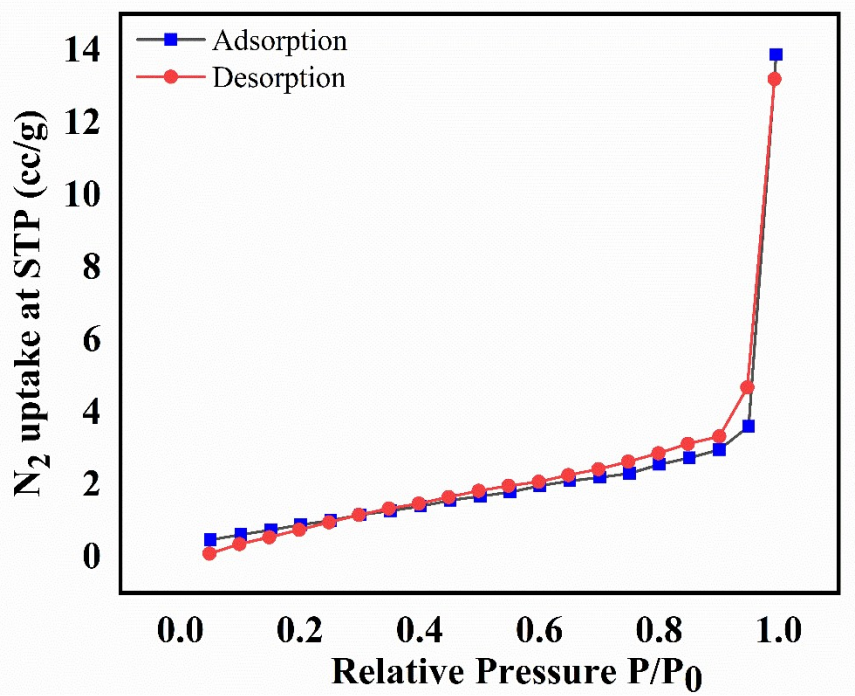

Figure S7. BET isotherm of **CuI-CP** using N_2 adsorption/desorption method .

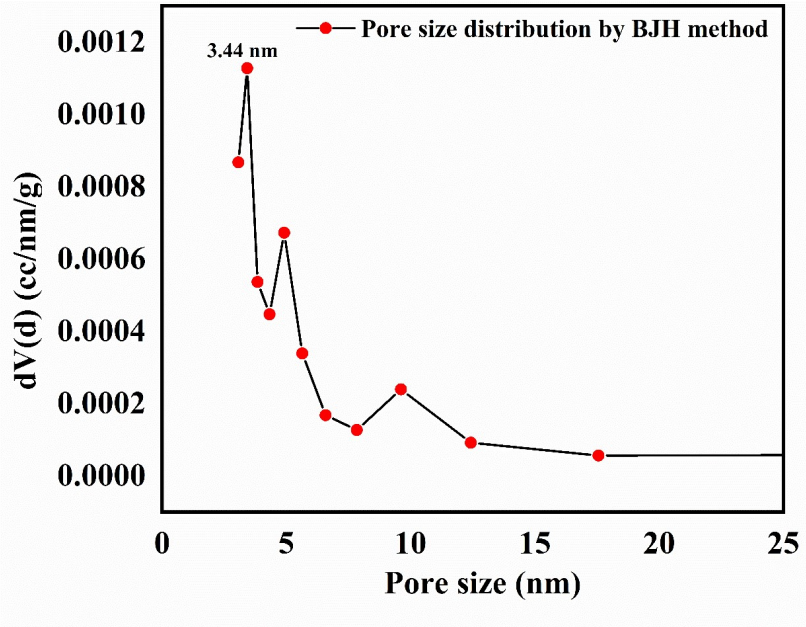

Figure S8. Porosity distribution by BJH method of **CuI-CP**.

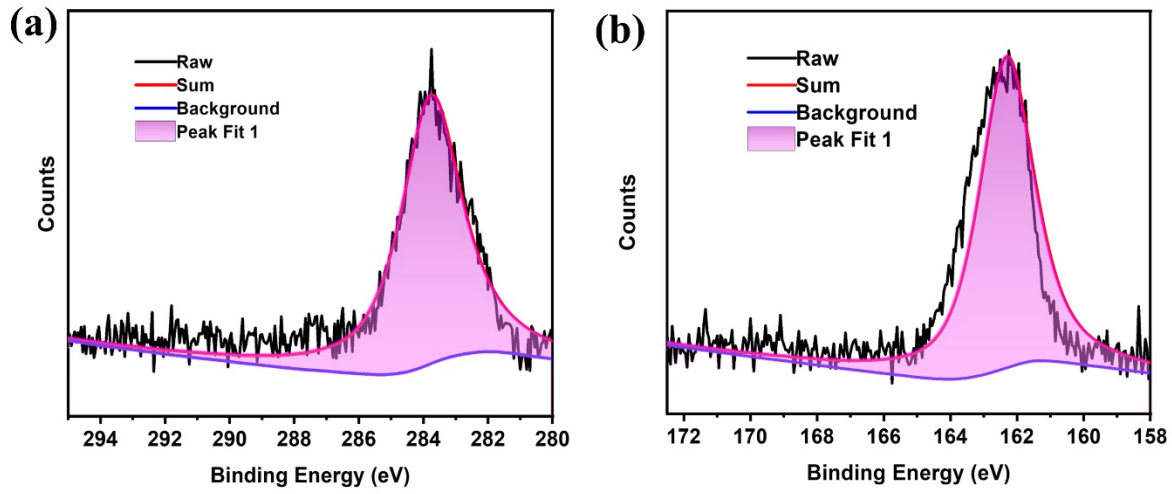

Figure S9. (a) XPS spectrum of C_{1s} and (b) XPS spectrum of S_{2p}.

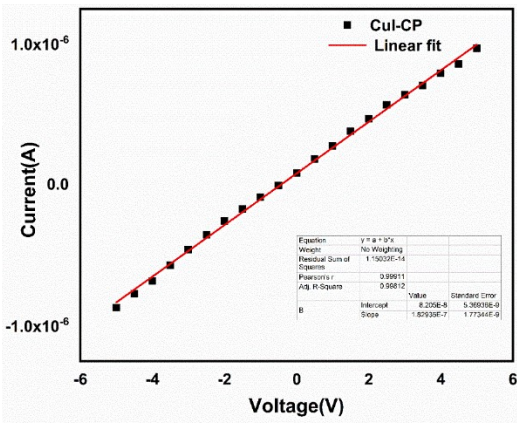

Figure S10. Electrical conductivity of **CuI-CP**.

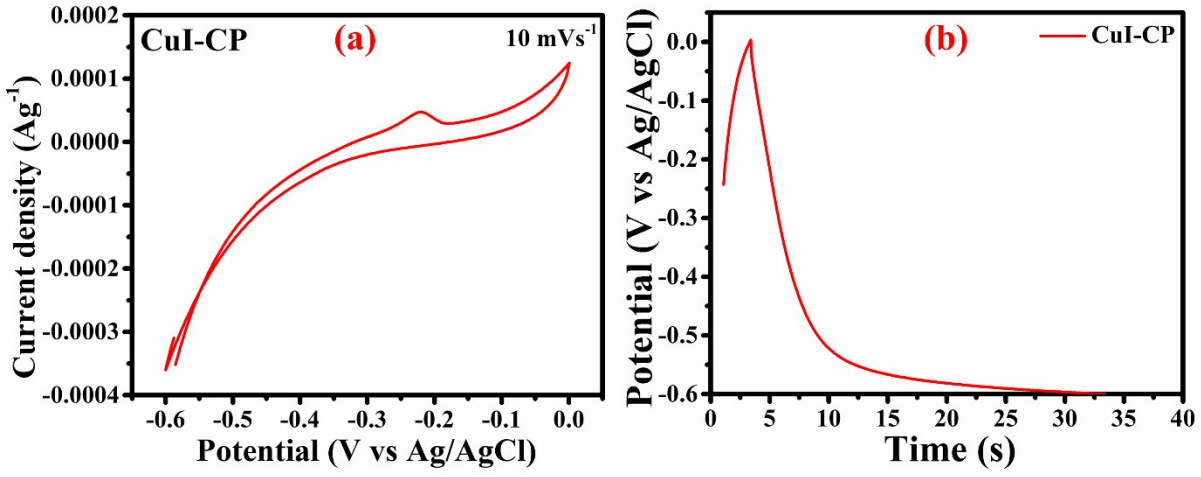

Figure S11. (a-b) . CV and GCD of **CuI-CP** in negative potential at 10 mVs^{-1} and 1 Ag^{-1} respectively.

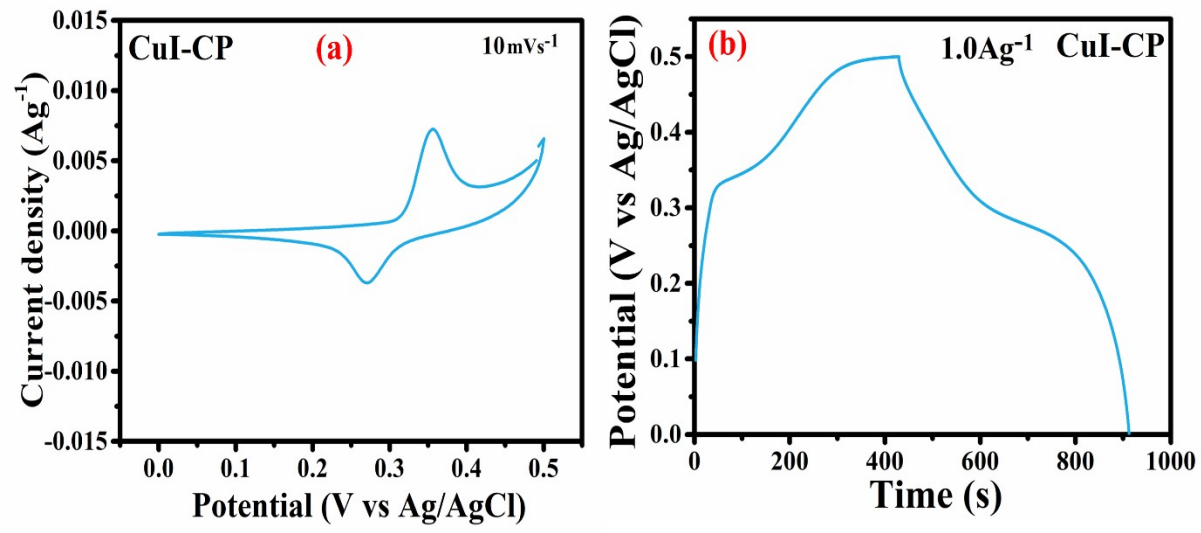

Figure S12. (a-b) CV and GCD of **CuI-CP** in positive potential at 10 mVs^{-1} and 1 Ag^{-1} respectively.

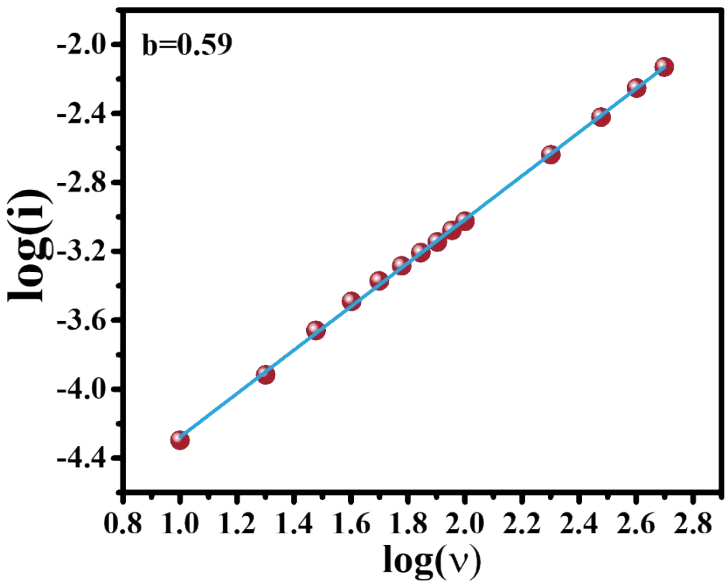

Figure S13. Charge storage kinetics: ln i vs. ln ν plots of **CuI-CP**. The slope of each plot represents the value of b.

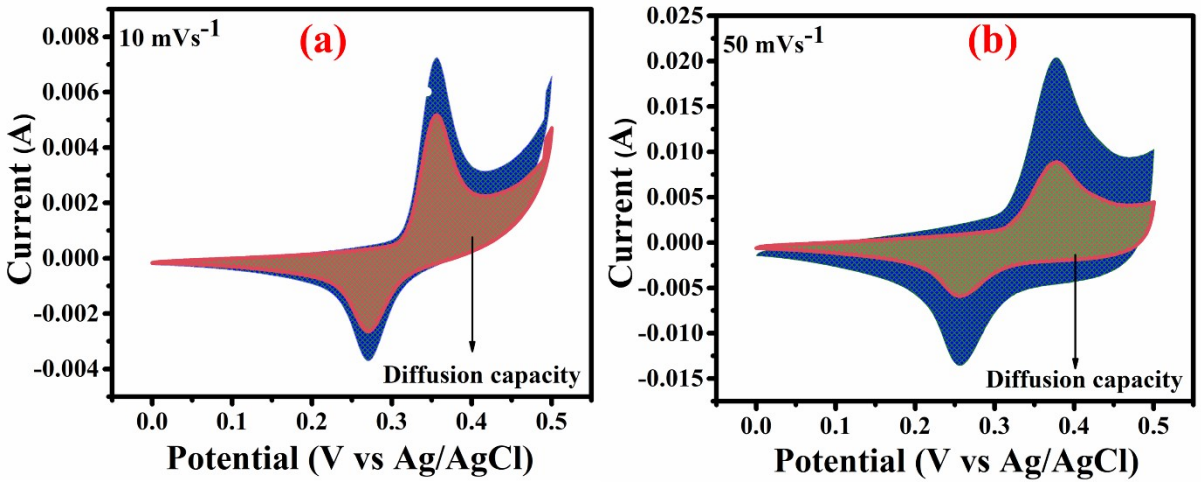

Figure S14. Comparison of calculated CV profile of **CuI-CP** for diffusion-only capacity and overall experimental at 10 mVs^{-1} and 50 mVs^{-1}.

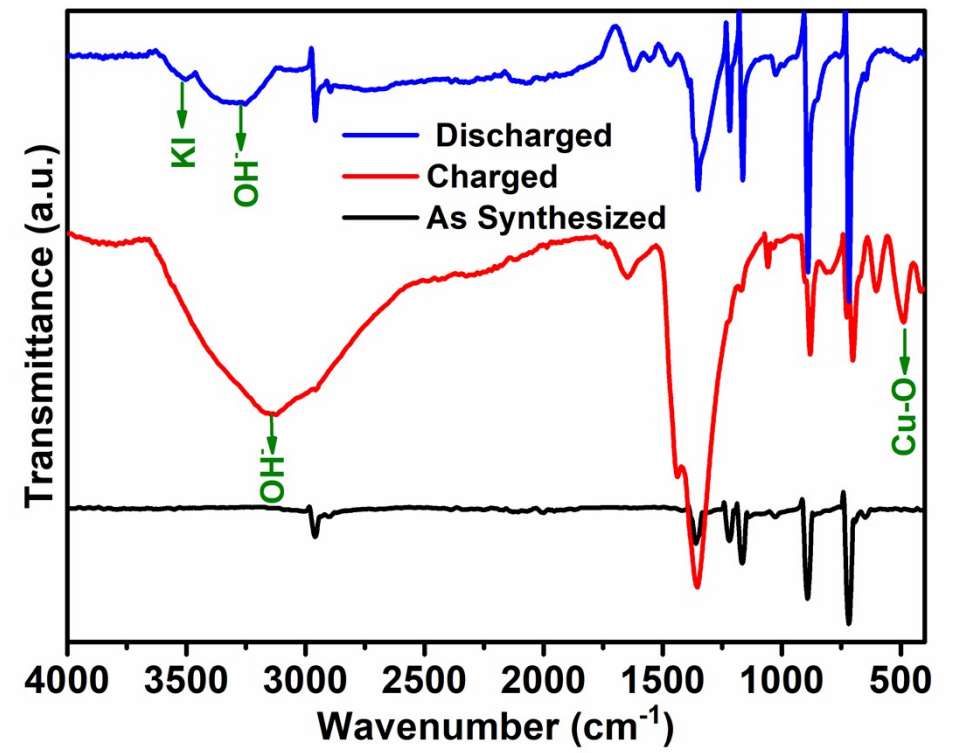

Figure S15. FT-IR of as-synthesized **CuI-CP**, charged state **CuI-CP** and discharged state **CuI-CP**.

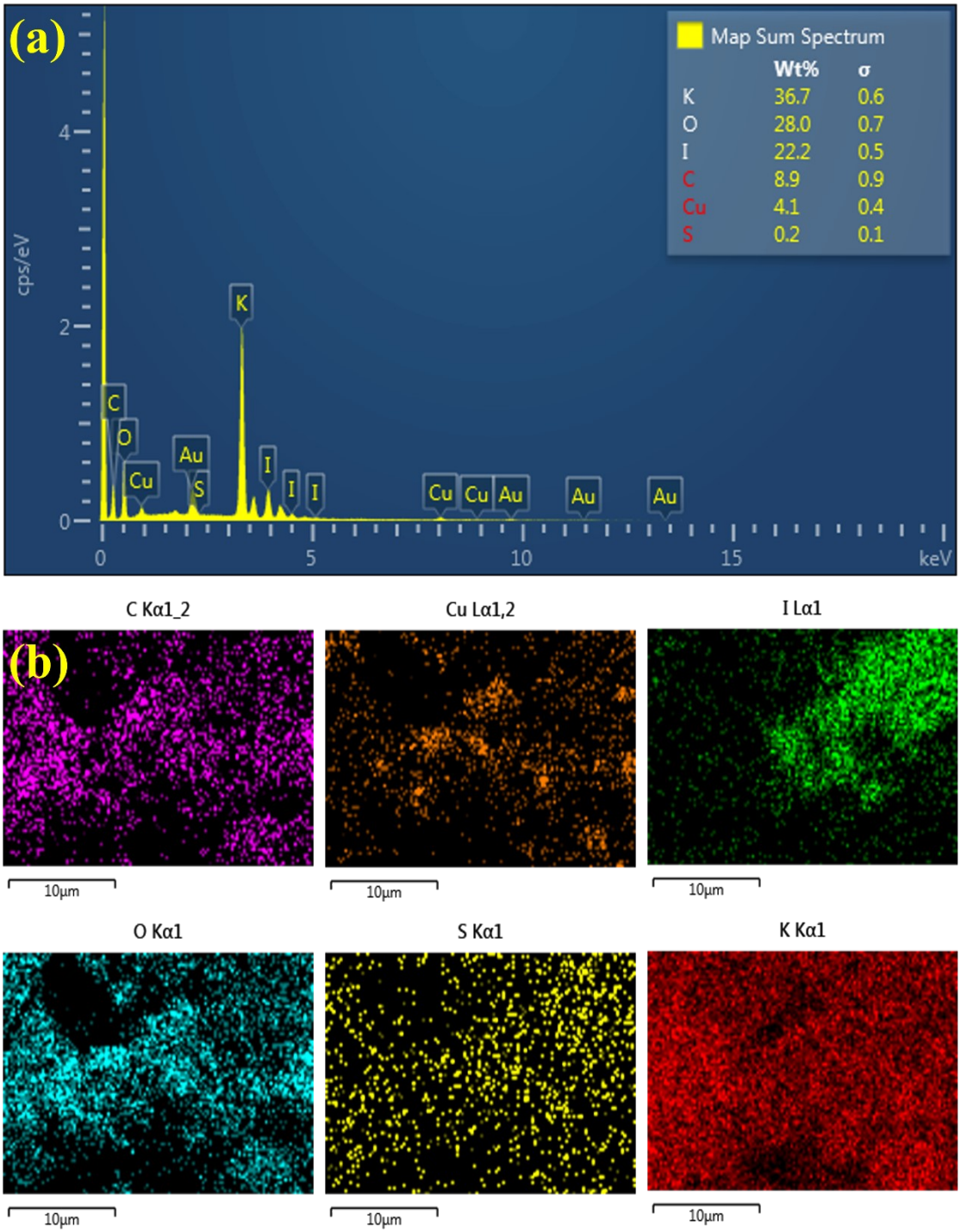

Figure S16 (a,b) EDS and elemental mapping of **CuI-CP** after cyclic stability.

Table S4. Comparison table for efficiency in devices.

Metal complex	Electrolyte	E_d (Wh Kg^{-1})	P_d (W Kg^{-1})	Voltage range (V)	Specific capacity /capacitance	Cycling stability	Ref.
Ni-MOF	6M KOH	90.3	1180	0-2	833.2 C g^{-1} @ 1 A g^{-1}	82%, 10000 cycles	[3]
Zn-MOF	6M KOH	83.0	1180	0-2	828.3 C g^{-1} @ 1 A g^{-1}	82%, 10000 cycles	[3]
Ni-MOF	2M KOH	50.1	2550	0-2	2.38 C cm^{-2} at 1 mA cm^{-2}	88%, 10000 cycles	[4]
Ni-MOF	6M KOH	57.1	800	0-2	1036 F g^{-1} @ 1 A g^{-1}	76%, 5000 cycles at 10 A g^{-1}	[5]
Ni-MOF	6M KOH	30.7	388.5	0-1.4	840 F g^{-1} @ 2 A g^{-1}	84%, 7000 cycles	[6]
$Ni_2[CuPc(NH)_8]$	1 M Na2SO4	51.6	32100	0-1.8	400 F g^{-1} @ 0.5 A g^{-1}	90.3 %, 5000 cycles	[7]
(Cu-TBC)	0.1M H_2SO_4	18.89	6000	0-0.6	474.8 F g^{-1} @ 0.2 A g^{-1}	83%, 5000 cycles at 5 A g^{-1}	[8]
$Ni_2[CuPcS_8]$	1 M $TEABF_4$/acetonitrile	57.4	23300	0-2.5	312 F g^{-1} @ 0.5 A g^{-1}	96.1%, 5000 cycles	[9]
Cu(I)CN- MOF	6M KOH	62.9	1100	0-2	266.5 C g^{-1} @ 1 A g^{-1}	81.1%, 5000 cycles	[10]
CuI -CP	**1M KOH**	**77**	**3080**	**0-1**	**498 C g^{-1} @ 1 A g^{-1}**	**93.8 %, 10000 cycles**	**This work**

References :

[1] O. V. Dolomanov, L. J. Bourhis, R. J. Gildea, J. a. K. Howard, H. Puschmann, *J Appl Cryst* **2009**, *42*, 339–341.

[2] G. M. Sheldrick, *Acta Cryst A* **2015**, *71*, 3–8.

[3] Z.-H. Ren, Z.-R. Zhang, L.-J. Ma, C.-Y. Luo, J. Dai, Q.-Y. Zhu, *ACS Appl. Mater. Interfaces* **2023**, *15*, 6621–6630.

[4] Y. Pan, Y. Han, Y. Chen, D. Li, Z. Tian, L. Guo, Y. Wang, *Electrochimica Acta* **2022**, *403*, 139679.

[5] X. Zhang, Z. Liu, X. Jin, F. Liu, X. Ma, N. Qu, W. Lu, Y. Tian, Q. Zhang, *Inorg. Chem.* **2023**, *62*, 7360–7365.

[6] R. Sahoo, S. Ghosh, S. Chand, S. Chand Pal, T. Kuila, M. C. Das, *Composites Part B: Engineering* **2022**, *245*, 110174.

[7] P. Zhang, M. Wang, Y. Liu, S. Yang, F. Wang, Y. Li, G. Chen, Z. Li, G. Wang, M. Zhu, R. Dong, M. Yu, O. G. Schmidt, X. Feng, *J. Am. Chem. Soc.* **2021**, *143*, 10168–10176.

[8] J. Zhao, T. Zhang, J. Ren, Z. Zhao, X. Su, W. Chen, L. Chen, *Chemical Communications* **2023**, *59*, 2978–2981.

[9] P. Zhang, M. Wang, Y. Liu, Y. Fu, M. Gao, G. Wang, F. Wang, Z. Wang, G. Chen, S. Yang, Y. Liu, R. Dong, M. Yu, X. Lu, X. Feng, *J. Am. Chem. Soc.* **2023**, *145*, 6247–6256.

[10] Z.-R. Zhang, Z.-H. Ren, C.-Y. Luo, L.-J. Ma, J. Dai, Q.-Y. Zhu, *Inorg. Chem.* **2023**, *62*, 4672–4679.